Astron. Astrophys. 335, 255–260 (1998)

ASTRONOMY
AND
ASTROPHYSICS

Van Hoof effect between metallic lines in RR Lyrae⋆

M. Chadid[1] **and D. Gillet**[2]

[1] GRAAL, CNRS, CC 72, Université Montpellier II, F-34095, Montpellier Cedex 05, France (chadid@graal.univ-montp2.fr)
[2] Observatoire de Haute-Provence CNRS, F-04870 Saint-Michel l'Observatoire, France (gillet@obs-hp.fr)

Received 24 November 1997 / Accepted 10 February 1998

Abstract. From theoretical models, it is now well known that the pulsation motion of atmospheric layers located above the photosphere have not the form of a standing wave especially in large amplitude pulsating stars such as RR Lyrae stars. In this paper, we report for the first time a weak but clear Van Hoof effect between some metallic lines in the atmosphere of the brightest RR Lyrae star of the sky: RR Lyrae. This shows that the propagation time of the pulsation wave through the atmosphere is now measurable with high resolution spectrographs. This provides a power tool to test nonlinear nonadiabatic pulsating models. We also confirm, but with a better accuracy, the Van Hoof effect with hydrogen lines which are formed higher in the atmosphere. Thus our observations put into evidence that large amplitude nonlinear motions of the atmospheric layers already exist at the photospheric level i.e., in the deep atmosphere.

Key words: hydrodynamics – shock waves – stars: pulsation – stars: variables: RR Lyrae – stars: individual: RR Lyrae

1. Introduction

In the pulsating stars, β Cephei, RR Lyrae, classical Cepheids and δ Scuti, a differential variation of the radial velocity of metallic lines and Balmer ones was observed. Several explanations are proposed (Mathias & Gillet 1993). The most important are a phase lag due to the propagation time of the wave between the different line forming regions, and a variation of the thermodynamical conditions in the line forming region.

Historically, this velocity difference was observed for the first time by Van Hoof and Struve (1953) in the β Cephei star β CMa. A similar lag was detected later in many β Cephei stars such as 16 Lac (Van Hoof et al. 1954), BW Vulpeculae (Mc Namara et al. 1955), σ Scorpii (Struve et al. 1955). Van Hoof effect was also observed in other pulsating star classes e.g., δ Scuti stars β Cas (Yang et al. 1982) and ρ Pup (Mathias et al. 1997), classical Cepheids (Wallerstein et al. 1992) and RR Lyrae stars RR Lyrae (Mathias et al. 1995, Paper I).

Recently, the Van Hoof effect has been studied in much more details, and even detected between several metallic lines in some pulsating stars: β Cephei star BW Vulpeculae and α Lupi (Mathias & Gillet 1993), δ Scuti stars 20 CVn (Mathias & Aerts 1996) and classical Cepheids (Wallerstein et al. 1992, Butler 1993). However, in RR Lyrae stars, no Van Hoof effect is observed between metallic lines. Mathias et al. (1995) interpreted the absence with the help of nonlinear nonadiabatic pulsational models of RR Lyrae itself (Fokin 1992). On one hand, they suggested that the absence is due to the fact that all metallic lines are formed in the same region, all relevant layers are then submitted, at approximatively the same time, to the same physical effects. On the other hand, strong shock waves only form in the high atmosphere where the hydrogen line cores are produced and not in the deep atmosphere where the metallic line cores are formed.

Recently, Chadid & Gillet (1996a, 1997) detected, for the first time, the line doubling phenomenon on two metallic absorption lines of the brighest RR Lyrae star: RR Lyrae. It was interpreted as the consequence of a "two-step" Schwarzchild's mechanism. A complete theoretical study was recently given by Fokin and Gillet (1997). Thus a strong shock wave propagates throughout the photospheric layers contrary to the initial Fokin's theoretical conclusion (1992). It is first receding, then stationary during a short time and finally advancing. Its amplitude varies with Blazhko phase approximately from a Mach number 4 to 6. Consequently, it is important to revise the fundamental question : does the Van Hoof effect exist between metallic lines in the RR Lyrae stars ?

The goal of this paper is devoted to the detection of this phenomenon. In Section 2 we describe the observations and the data reduction process. The detection of the Van Hoof effect is performed in Sect. 3 and discussed in Sect. 4. Finally, the last section is devoted to some general concluding remarks.

2. Observations and data reduction

Spectroscopic observations used in this study were obtained with the new, cross-dispersed spectrograph ELODIE at the 1.93-m telescope at Observatoire de Haute-Pro- vence (Baranne et al. 1996). The detector used is a thinned Tk 1024 CCD, with 1024 x 1024 elements of size 24 μm^2.

The observations were obtained during three consecutive nights from the 3rd to 5th of August 1994 (see Tables 1 and 2

⋆ Based on observations obtained at the Observatoire de Haute-Provence (France)

in Chadid & Gillet 1996, Paper II). The spectral domain ranges from 3900 Å to 6800 Å with a resolving power $R \simeq 42,000$, a signal-to-noise ratio S/N around 50 for an exposure time between 5-10 mn giving a time resolution around 1% of the pulsation period (13 h 36 mn). The description of the data reduction can be found in Paper II. Yet, the phasing of the observations in Paper II are only approximative because we did not have simultaneous photometry. After, we corrected this phasing (Chadid & Gillet 1997). The blazhko phase of these observations is $\psi = 24.98$ while the pulsation phase is approximately similar with those of Paper II (shift of 0.04).

Heliocentric radial velocities were determined from a gaussian fit on the whole profiles, except for Hα, because due to well-marked Stark wings and blends, only the Hα-core was considered. Moreover, because during the hump phase, hydrogen and some metallic lines show a doubling line structure, consequence of the shock wave propagation (see Chadid & Gillet 1996a, 1997). The bottom of the line forming region is rising (blue component) due to the strong outward wave, while its top is still falling (red component) according to the ballistic motion. Hence, since we are interested in the wave propagation along the radial axis, we only constructed the hydrogen and some metallic velocity curves associated with the blue components. This latter was measured using the Munich Image Data Analysis System (MIDAS).

3. Van Hoof effect between metallic lines

3.1. Detection

In Paper I, we had not detected a Van Hoof effect between the metallic lines Fe II $\lambda\lambda$ 4923.921 and Fe I $\lambda\lambda$ 4920.509 using observations done with the AURELIE spectrograph (resolving power of 17,000 and a temporal resolution of 5%). Our new observations with the spectrograph ELODIE are shown Figs. 1-2. From the velocity-velocity diagram, it is clear that a variable phase shift is present between these two lines and consequently, for the first time, we confirm the detection of a metallic Van Hoof effect.

Note that to obtain Fig. 2, we have done a selection of our data, which were collected over three consecutive nights, to make up a complete pulsation period: from $\varphi = 0.774$ to 0.108 for August 3rd, 1994, from 0.197 to 0.700 for August 5th, 1994 and from 0.714 to 0.766 for August 4th, 1994 (see Fig. 1 of Paper II). Due to the presence of a Blazhko effect a small velocity shift must be expected from one night to the following. For instance, it is around 0.6 km/s from August 4th to August 5th, 1994 for the Fe II line. Consequently, this effect must be smaller than the amplitude of the observed shifts in Figs. 2–5. Another effect, due to the non-strict reproducibility of the atmospheric dynamics above all the photosphere, is certainly the main cause of dispersion of radial velocities from one cycle to the following.

In Fig. 2, each point represents an individual spectrum. The average accuracy is certainly better than 500 m/s. Consequently, the two closed loops are certainly real. From approximately phase 0.43 to 0.94 i.e., during the atmospheric compression,

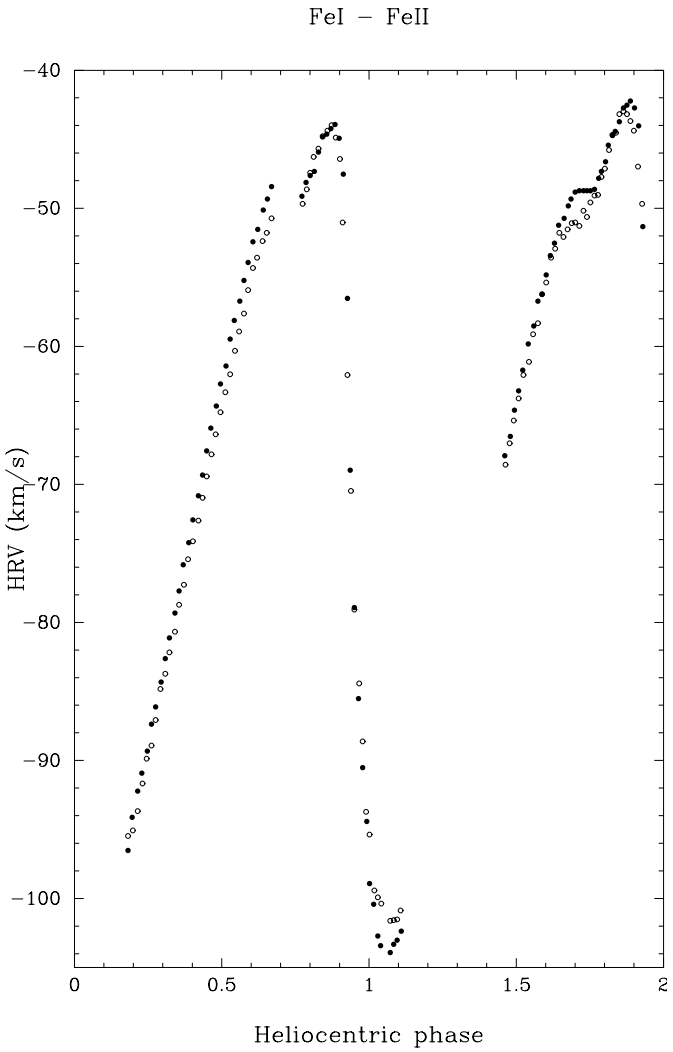

Fig. 1. Heliocentric radial velocity curves of Fe II $\lambda\lambda$ 4923.921 (black points) and Fe I $\lambda\lambda$ 4920.509 (white points) obtained over three consecutive nigths 3rd, 4th and 5th August, 1994 with the spectrograph ELODIE

the upper loop is described anti -clockwise. This means that the variation of the Fe II velocity curve is late compared to those of Fe I one (see Fig. 1). Then, during the expansion, from phase 0.94 to 0.43, the lower loop is described clockwise, showing that now the Fe I velocity curve is late with respect to the Fe II one. Note that the maximum amplitude of these two velocity curves are about the same.

Contrary to pulsating stars with very weak amplitude and showing almost sinusoidal velocity curves (see for instance Mathias & Gillet 1993), the complicated shape of the velocity-velocity diagram for these iron metallic lines indicates that the velocity shift between these two lines is phase-dependent. This is consistent with the fact that, for large amplitude pulsating stars, the motion of atmospheric layers above the photosphere is far away from that of a standing wave (Fokin & Gillet 1997). Consequently, except the detection of the Van Hoof effect, it

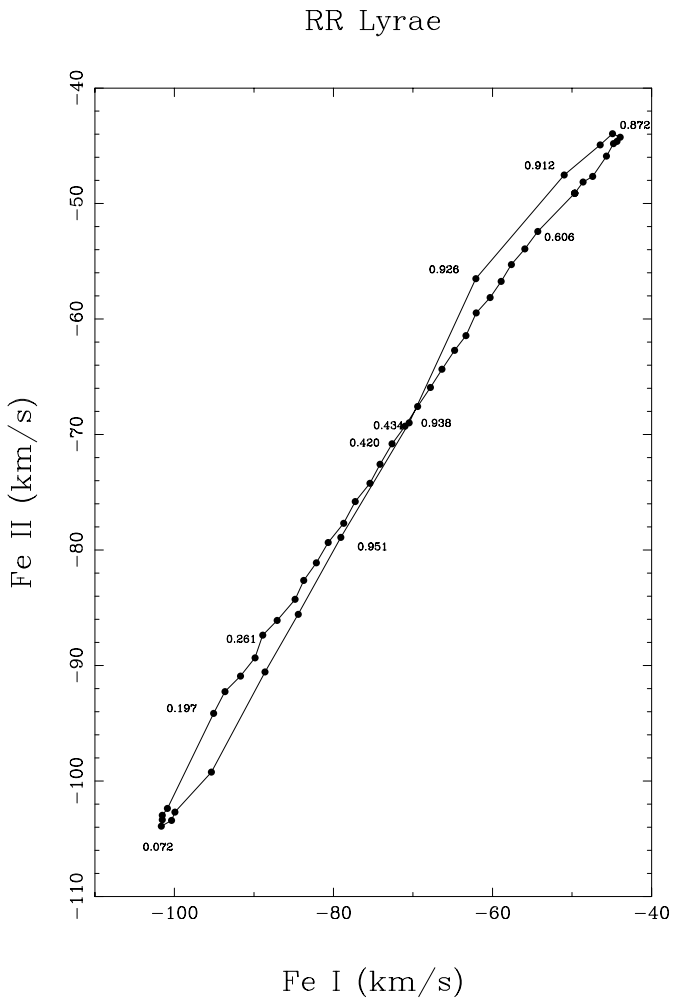

Fig. 2. The heliocentric radial velocity curve of Fe II $\lambda\lambda$ 4923.921 is represented versus that of Fe I $\lambda\lambda$ 4920.509. On the resulting curve is indicated the pulsation phase, according to the ephemeris given in Sect. 2

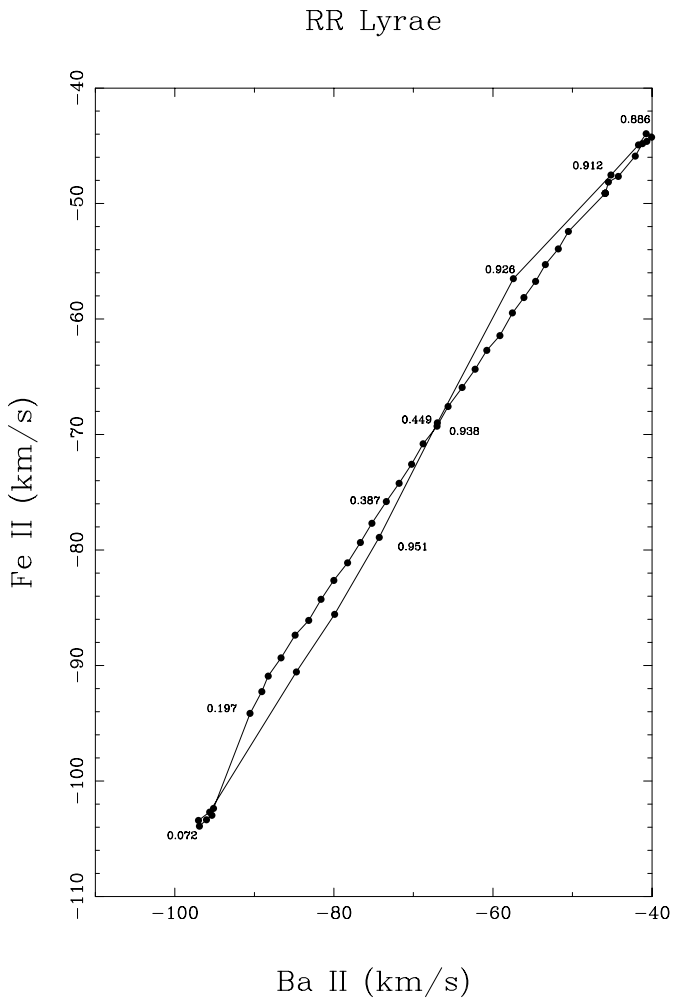

Fig. 3. Same as Fig. 2, but for Fe II $\lambda\lambda$ 4923.921 and Ba II $\lambda\lambda$ 4934.076

is difficult to deduce additional reliable information from this kind of velocity-velocity diagrams.

Figs. 3-4 show respectively the velocity-velocity diagrams for Ba II $\lambda\lambda$ 4934.076 and Ti II $\lambda\lambda$ 5188.700 lines always with respect to the Fe II $\lambda\lambda$ 4923.921 line. These curves are similar to the Fe I-Fe II curve (Fig. 2).

Note that the line doubling (or broadening) phenomenon (see Paper II), occurring within the phase interval 0.90-0.95, has an effect on the shape of the velocity-velocity curve. In all above figures, the velocity was measured with a gaussian fit over the full line without taking into account the doubling. Fig. 5 shows how the velocity-velocity curve changes when only the blueshifted line component is considered. A gaussian fit with two components was performed on the observed profile during this phase interval. We know that, when the line forming region is traversed by a shock wave, the relevant layers are divided in to two groups of opposite motion. Moreover, when the shock is propagating outward in the atmosphere, their two density columns are extremely variable, like the corresponding absorption components. Thus the last diagram (Fig. 5) always allows to follow only one type of the atmospheric motion (expansion or contraction). Three loops become visible showing again that in fact the atmospheric motion is very complicate.

3.2. Interpretation

One of the best way to get a physical understanding of the Van Hoof effect is to proceed to the analysis of the differential curves of velocity, radius separation and acceleration of the two elements as previously done (see Paper I). Fig. 6a–c shows these three curves for Fe I-Fe II lines presented above. The stellar restframe velocity $\dot{R}$ is given by

$$\dot{R}(\varphi) = -p(V(\varphi) - V_*) \quad (1)$$

where $V(\varphi)$ is the heliocentric radial velocity, V_* the stellar restframe velocity and p the geometrical projection and limb-darkening correction factor. The velocity difference

$$\Delta V = \Delta\dot{R} \equiv \dot{R}_{Fe\,I} - \dot{R}_{Fe\,II} \quad (2)$$

does not depend on the estimated value of V_*. ΔV is only affected by the accuracy of the laboratory wavelength of each

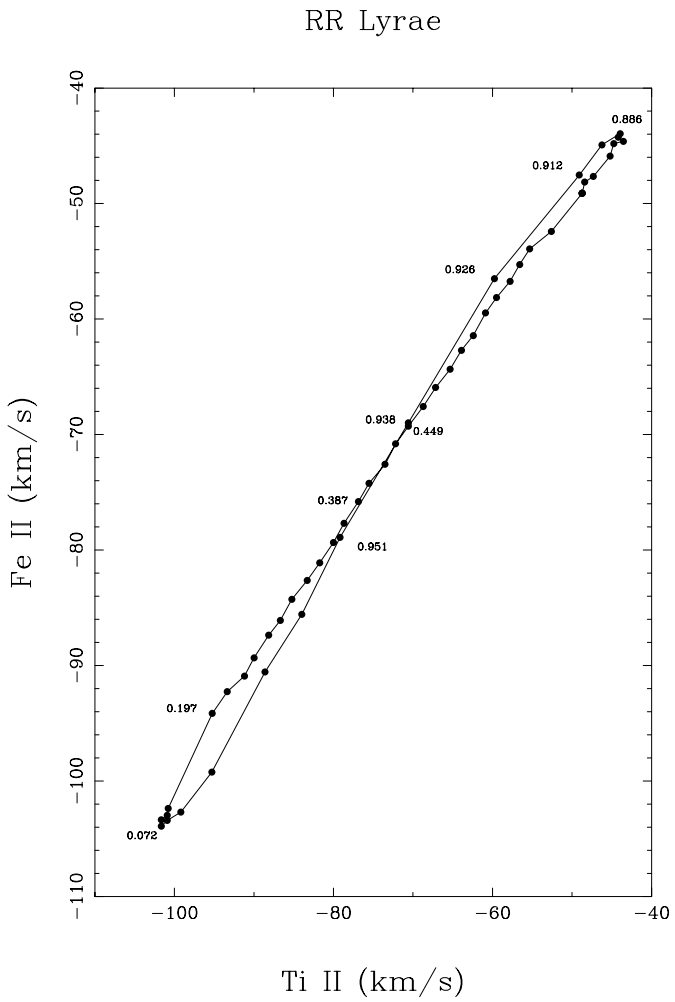

Fig. 4. Same as Fig. 2, but for Fe II $\lambda\lambda$ 4923.921 and Ti II $\lambda\lambda$ 5188.700

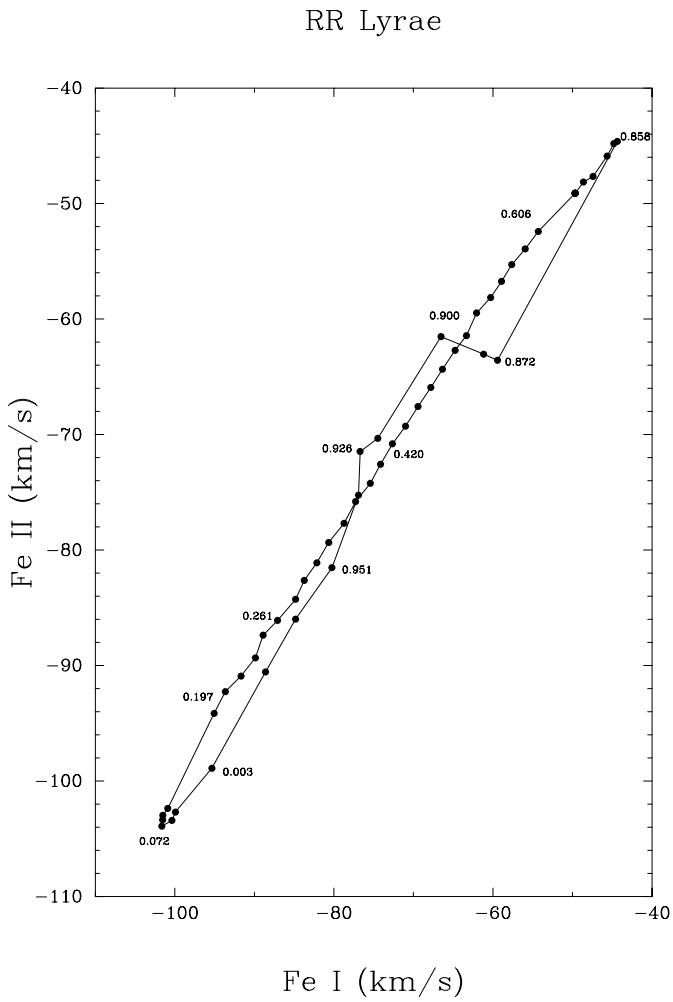

Fig. 5. Same as Fig. 2, but when only the blueshifted absorption component is taken into account when the line doubling is present

absorption line and by the adopted p-value. Note that an error of 0.1 Å on one wavelength introduces a velocity shift of 0.6 km/s. Thus we expect that the ΔV-curve can be more or less shifted from its real position by less than 1 km/s. Although we have taken a constant p-value equal to 1.36, this shift is probably phase dependent because p varies during the pulsation (Sabbey et al. 1995).

From pulsation phase $\varphi = 0.42$ (maximum radius) to $\varphi = 0.64$ (middle of the contraction), Fe I and Fe II line forming regions have the same variation of their acceleration (Fig. 6a–cc). They are not equal because the differential radius linearly increases during this phase interval (Fig. 6a–cb). If we accept, as shown by the Fokin's model, that the Fe II line is formed higher than the Fe I line during the expansion, then the average distance between these two regions is near $0.05\,R_\odot$ between phases 0.42 and 0.64 i.e., 50% of their maximum separation. During this time, the differential radial velocity only increases by 1 km/s. It can be surprising that the average separation between Fe I and Fe II increase during the contraction. In fact, and as shown by theoretical models (Fokin & Gillet 1997), the motion of atmospheric layers already above the photosphere is extremely nonlinear for a star such as RR Lyr. A series of rarefactions and compressions can occur at the same time on the line of sight due to the complicated ballistic process.

From $0.64 < \varphi < 0.77$, i.e., just before the photospheric minimum radius, the differential acceleration of the Fe line forming regions begins to decrease (up to 0.5 m/s^2) because they penetrate more and more in the dense photosphere, slowing down their free fall motion. Because Fe II is expected to be formed higher, the deceleration is first stronger for Fe I layers than for Fe II ones. This effect becomes visible near phase 0.77, because the differential velocity and radius are decreasing (Figs. 6a–ca and b). Until this phase, the Fe I velocity was a little bit larger than the Fe II velocity. Both differential acceleration and radius reach a maximum at phase 0.77 when the Fe I velocity becomes smaller than the Fe II one and then begins to decrease. This is the consequence of the progressive increase breaking induced by the dense atmosphere during the contraction. All these effects occur during the secondary photospheric acceleration centered at about phase 0.77 in our Fe I and Fe II acceleration curves (not shown here). A stillstand is also visible in the radial velocity curve at this phase (Paper II). Fokin & Gillet (1997) showed that a shock wave (s3) produces at this

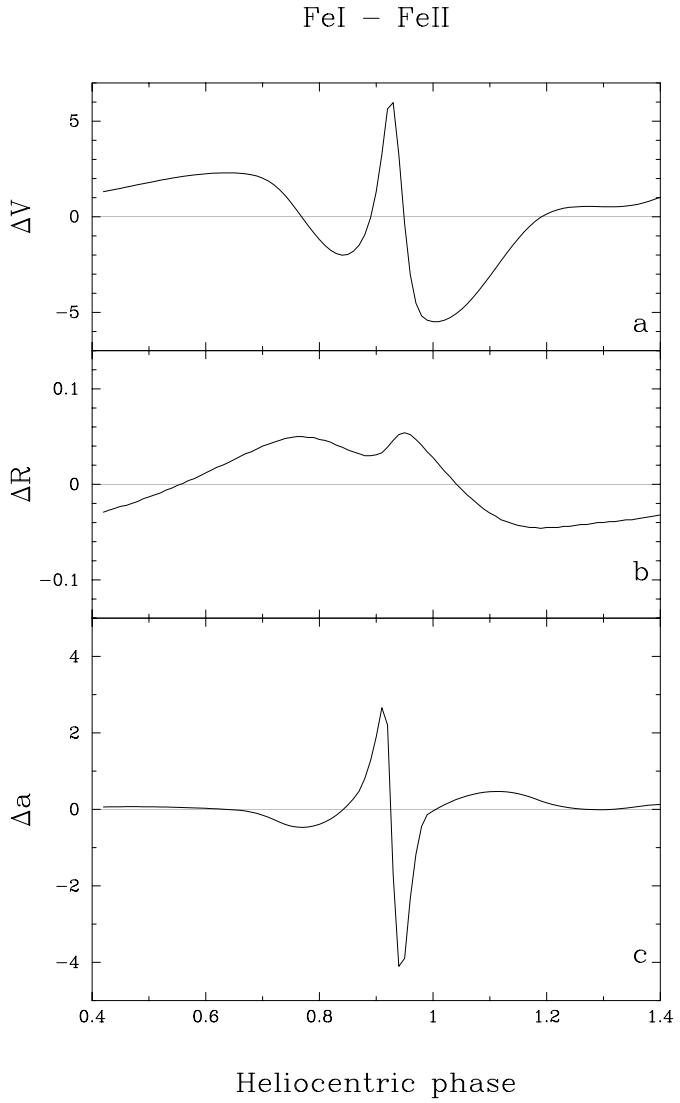

Fig. 6a–c. Differential velocity ΔV, radius ΔR and acceleration Δa between Fe I $\lambda\lambda$ 4920.509 and Fe II $\lambda\lambda$ 4923.921 lines. **a** $\Delta V = \dot{R}_{\rm Fe\,I} - \dot{R}_{\rm Fe\,II}$ [km.s^{-1}]. **b** $\Delta R = \int \Delta V {\rm d}\varphi$ [R$_\odot$]. **c** $\Delta a = \frac{\rm d}{{\rm d}\varphi}(\Delta V)$ [m.s^{-2}]

time an additional local compression of the atmospheric layers in which metallic lines are formed. This shock was called the "early shock" by Hill (1972) who was the first to detect it in his nonlinear pulsating model.

Near phase 0.93, a strong peak appears within the differential velocity curve (Fig. 6a–ca). In the same time the differential acceleration curve shows a rapid sign inversion, here from positif to negatif (Fig. 6a–cc). These two features correspond to the occurrence of two close strong shocks (s1 and s2) which traverse the photospheric layers at this phase (see Fokin & Gillet 1997). The star radius is minimum and the atmospheric compression is maximum. Because the differential acceleration is first increasing, this means that the Fe I layers, located a little bit deeper than the Fe II layers, are first affected by the shocks. A very short delay between 0.01 and 0.02 in phase is expected.

The expansion appears just after the passage of the shocks s1 and s2 across the photosphere ($\varphi = 0.94$, Fokin & Gillet 1997). The Fe I and Fe II velocities become positive. After to have reached a second maximum at $\varphi = 0.94$, ΔR is now decreasing in spite of the atmospheric expansion. This is certainly due to the fact that the forming Fe I and Fe II regions have been strongly affected by the passage of the radiative shock waves s2 and s1 but not at the same rate. For instance, a compression rate of 10 or more is expected depending of the shock Mach numbers. This effect is very sensitive to the shock velocity, therefore to its altitude. Thus, although the atmospheric expansion is strongly growing, the relaxation of the shock compression certainly needs an appreciable time as indicated by the long decreasing tail (until $\varphi = 1.10$) of the ΔR curve (Fig. 6a–cb). Also, the differential velocity ΔV notably changes during this phase interval. The two iron layers do not have a constant differential velocity before phase 1.25. After, during the end of the expansion i.e., up to the maximum radius ($\varphi = 0.42$), the pulsation motion is almost a standing wave.

The two other metallic lines (Ba II and Ti II) discussed in Sect. 3.1 show the same kind of differential curves. The Ti II-Fe II and Fe I-Fe II curves are very similar indicating that the Ti II and Fe I elements are almost formed at the same altitude as confirmed by a detailed calculation (Fokin, private communication). The Ba II-Fe II curve presents a narrower velocity and acceleration peaks and a very small depression near phase 0.9. This means that the Ba II line is formed closer of the Fe II line than Fe I and Ti II ones as calculated.

4. Van Hoof effect with hydrogen

Fig. 7a–c gives the Hα-Fe II differential curves. They are similar to those obtained in Paper I except that all amplitudes are quite larger. Indeed ΔV reaches 134 km/s instead 40 km/s in Paper I, while for ΔR we have respectively 1.43 R$_\odot$ and 0.28 R$_\odot$ and for Δa, 155 m.s^{-2} and 22 m.s^{-2}. It is true that the values of Paper I were given for Hβ which is formed a little bit lower but we can conclude that these new amplitudes appear considerably larger with our new observations. Apart from a double resolving power, their time resolution is 5 times better. Consequently an effective average effect affects our first observations (July 1990) and certainly explains in part this large difference in amplitude. In any event, this demontrates well the importance of obtaining high quality data.

5. Conclusions

The observations presented in this paper show that a phase lag between metallic lines is present during the pulsation of RR Lyr. It is small (between 1 and 2%) but, due to the high quality of our observations, it is clearly established. Thus, this observational result, reveals for the first time that the pulsation motion of the atmospheric layers localised just above the photosphere have the form of a running wave. Its amplitude is certainly appreciable, since for instance, the distance between two metallic layers is strongly variable and increases during the contraction.

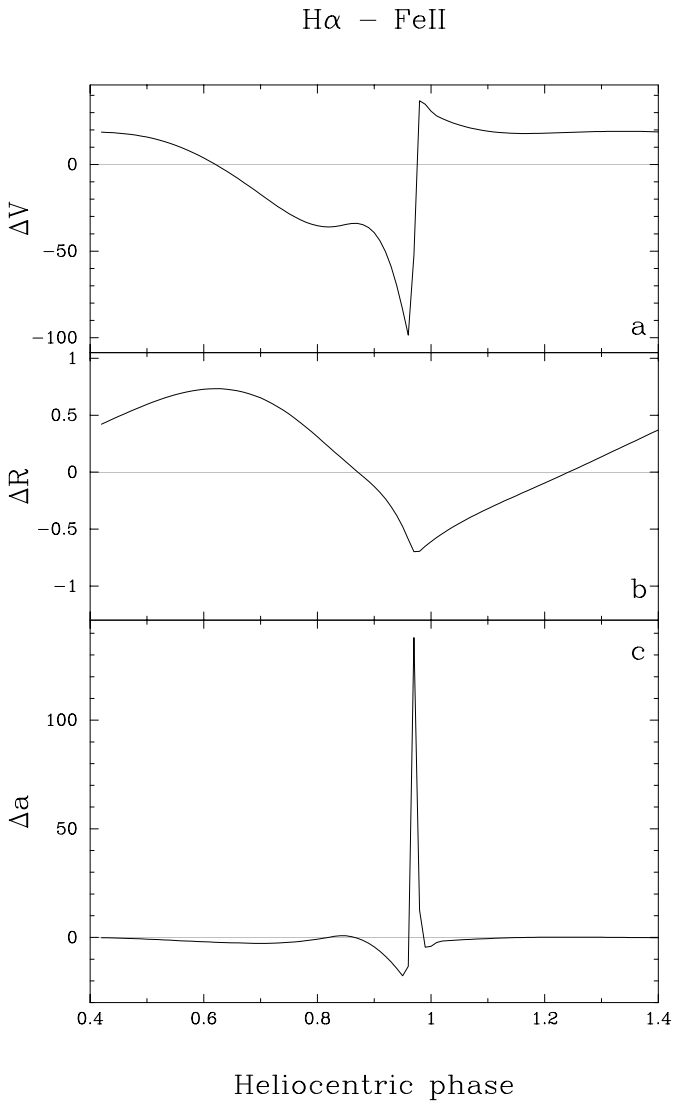

Fig. 7a–c. Differential velocity ΔV, radius ΔR and acceleration Δa between Hα $\lambda\lambda$ 6562.817 and Fe II $\lambda\lambda$ 4923.921 lines. **a** $\Delta V = \dot{R}_{\mathrm{H}\alpha} - \dot{R}_{\mathrm{Fe\,II}}$ [km.s^{-1}]. **b** $\Delta R = \int \Delta V \mathrm{d}\varphi$ [R$_\odot$]. **c** $\Delta a = \frac{\mathrm{d}}{\mathrm{d}\varphi}(\Delta V)$ [m.s^{-2}]

Some effects associated with the three main shock waves detected in nonlinear pulsating models (Fokin & Gillet 1997), are observed within our new data. This confirms that the deep atmosphere of RR Lyrae, and certainly more generaly of RR Lyrae stars, is strongly affected by the nonlinear behaviour of the pulsation. In particular, the so-called "early shock", first theoreticaly discovered by Hill (1972), is indirectly detected by our observations.

This type of high quality observation provide us with a new opportunity to investigate the atmospheric structure of pulsating atmospheres of relatively large amplitude but also to give a new quantitative tool to check theoretical results of nonlinear models.

Acknowledgements. The authors would like to express their sincere thanks to Drs. A.B. Fokin and P. Mathias for valuable discussions on some aspects of this paper and for their constructive help. The work of MC has been done during the first year of a CNRS-post-doc fellowship (Centre National de la Recherche Scientifique, France).

References

Baranne, A., Queloz, D., Mayor, M., Adrianzyk, G., Knispel, G., Kohler, D., Lacroix, D., Meunier, J.-P., Rimbaud, G., Vin, A., 1996, A&AS 119, 373
Butler, R.P., 1993, ApJ 415, 323
Chadid, M., Gillet, D., 1996a, A&A 308, 481 (Paper II)
Chadid, M., Gillet, D., 1996b, A&A 315, 475
Chadid, M., Gillet, D., 1997, A&A 319, 154
Fokin, A.B., 1992, MNRAS 256, 26
Fokin, A.B., Gillet, D., 1997, A&A 325, 1013
Hill, S.J., 1972, ApJ 178, 793
Mathias, P., Gillet, D., Aerts, C., Breitfellner, M.G., 1997, A&A in press
Mathias, P., Aerts, C., 1996, A&A 312, 905
Mathias, P., Gillet, D., Fokin, A.B., Chadid, M., 1995, A&A 298, 843 (Paper I)
Mathias, P., Gillet, D., 1993, A&A 278, 511
Mc Namara, D.H., Struve, O., Bertiau, F.C, 1955, ApJ 121, 326
Sabbey, C.N., Sasselov, D.D., Fieldus, M.S., Lester, J.B., Venn, K.A., Butler, R.P., 1995, ApJ 446, 250
Struve, O., Mc Namara, D.H., Zebergs, V., 1955, ApJ 122, 122
Van Hoof, A., Struve, O., 1953, PASP 65, 158
Van Hoof, A., De Ridder, M., Struve, O., 1954, ApJ 120, 179
Wallerstein, G., Jacobsen, T.S., Cottrell, P.L., Clark, M., Albrow, M., 1992, MNRAS 259, 474
Yang S., Walker, G.A.H., Fahlman, G.G, Campbell, B., 1982, PASP 94, 317
Zakrzewski, B., 1996, in rocznik [Yearbook] Astron. Obs. Krakow., Intern. Suppl. No. 67, Krakow, page 119